Fluctuations and the resistive transition in paramagnetically limited superconductors

Koya Aoi*
Institut Max von Laue-Paul Langevin, 8046 Garching bei München, Germany

R. Meservey and P. M. Tedrow
Francis Bitter National Magnet Laboratory,† Massachusetts Institute of Technology, Cambridge, Massachusetts 02139

(Received 27 June 1973)

We have studied, both theoretically and experimentally, the extra conductivity σ_{fl} due to thermal fluctuations in high-field superconductors in the Pauli-paramagnetic limit (SPPL). We first investigate theoretically the Aslamazov-Larkin (AL) term, and show that the Pauli-paramagnetic effect in the AL term can be included by renormalizing the thickness of the film. Then we calculate the pair-breaking function for the Maki-Thompson (MT) term in a magnetic field within the lowest-order approximation of Keller and Korenman and show that in contrast to ordinary superconductors the MT term in SPPL can be enhanced by a weak parallel field. We also report the first experimental measurements of σ_{fl} in SPPL. The angular dependence of the AL term is found to be essentially in agreement with the calculation of Aoi reported earlier. Near T_{c0} the MT term is observed to be suppressed by a parallel field. We also study the effect of a perpendicular field, and find, both theoretically and experimentally, that in SPPL the MT term appears to be suppressed by a perpendicular field.

I. INTRODUCTION

In the past few years much effort has been devoted to the study of thermal fluctuations of the superconducting order parameter.[1–18] It has been found that fluctuations can give measurable effects on various properties of metals near the transition point. In the case of electrical conductivity, the extra conductivity σ_{fl} due to fluctuations is given as the sum of the Aslamazov-Larkin (AL) contribution[1] and the Maki-Thompson (MT)[2,4] contribution:

$$\sigma_{fl} = \sigma_{AL} + \sigma_{MT} \quad . \tag{1}$$

For two-dimensional superconductors σ_{AL} and σ_{MT} are given (in units where $\hbar = 1$) by

$$\sigma_{AL} = e^2/16\,d\tau \tag{2}$$

and

$$\sigma_{MT} = \left(\frac{e^2}{8\,d}\right)\frac{\ln(\tau/\delta)}{(\tau-\delta)} \quad , \tag{3}$$

where d is the thickness of the film, $\tau = \ln(T/T_{c0}) \approx (T/T_{c0}) - 1$, and T_{c0} is the transition temperature in zero field. Thompson[4] obtained Eq. (3) by introducing a pair-breaking parameter δ to remove the divergence of the Maki diagram. Kajimura and Mikoshiba[11] found that their experimental data could be well fitted to Eqs. (1)–(3) by choosing

$$\delta = 6\times10^{-4}R_{\square} \tag{4}$$

for their aluminum films, where $R_{\square}$ is the resistance in ohms per square of the film in the normal state. It was shown by Keller and Korenman[13] (KK) and by Patton[14] from microscopic calculations that the form of Eq. (3) is approximately correct in a restricted temperature range, but that δ is strongly temperature dependent[13]:

$$\delta = 2.1\times10^{-5}R_{\square}/\tau \quad . \tag{5}$$

This nonvanishing δ was obtained by modifying the BCS interaction with a vertex correction caused by the superconducting fluctuations themselves.

Magnetic field effects have been considered by many authors.[4–12] It is well known both theoretically[4] and experimentally[9,11,12] that a parallel field enhances the pair-breaking parameter δ and consequently suppresses σ_{MT} in superconductors in which the orbital motion of electrons limits $H_{c\parallel}$. On the other hand, it is predicted theoretically that a perpendicular field should enhance σ_{AL} so that in the neighborhood of T_c it is four times σ_{AL} in zero field. In the temperature range of τ' which is less than a few times δ, σ_{MT} should also be enhanced by a perpendicular field $\{\tau' = [T - T_c(H_\perp)]/T_c(H_\perp)$ is the reduced temperature difference$\}$. If the pair-breaking effect due to other mechanisms is small compared with that due to the perpendicular field itself, σ_{MT} near T_c can be as large as four times σ_{AL} in zero field.[4] The enhancement in a perpendicular field comes from the fact that the energy spectrum of the fluctuating pairs is discrete due to the Landau quantization, and that there is a large degeneracy in the lowest energy level $n = 0$. This degeneracy is to be compared with the zero- or parallel-field case where there is only one lowest energy state, namely, the $q = 0$ state (q is the wave vector of the fluctuation mode). The degeneracy in the perpendicular field case makes thermal fluctuations easier. There are relatively few experimental data available for the perpendic-

ular field case.[10,12,15] Aomine and Rinderer[12] observed that in the vicinity of the transition temperature, the fluctuation conductivity of Al is enhanced by no more than 20% over the zero-field value and that the MT contribution is suppressed by a perpendicular field. The latter is consistent with the measurements of Klenin and Crow.[15]

If the film is sufficiently thin (typically $d \lesssim 50$ Å for Al), the critical field $H_c(\theta)$ is limited by Pauli paramagnetism for small $\theta \ll \frac{1}{2}\pi$.[19,20] (We shall refer to such superconductors as SPPL, superconductors in the Pauli-paramagnetic limit.) Here θ is the angle between the film surface and the applied magnetic field. One might expect that the behavior of SPPL in a magnetic field is different from ordinary superconductors in which $H_c(\theta)$ is limited by the orbital motion of the electrons. In fact SPPL do show some percularities. For example, at low temperatures ($T \ll T_{c0}$) they undergo a first-order phase transition to the normal state with an increasing parallel magnetic field if the spin-orbital scattering rate is small.[20] However, there are cases in which the Pauli paramagnetism is completely implicit, although important. For example, in the angular dependence of the critical field $H_c(\theta)$, Tinkham's formula, which was derived without taking into account Pauli paramagnetism, works for SPPL.[21] This is because "the effective pair-breaking strength" due to the Pauli spin is quadratic in H, the same field dependence as that due to the orbital motions in a parallel field.

Fluctuations in SPPL were first considered by Fulde and Maki[16] for the parallel and perpendicular field cases and then extended by Aoi,[17] (hereafter referred to as I), to the cases of arbitrary field orientations. These authors considered only the AL contribution, assuming in agreement with the above-mentioned experiments that the MT contribution is suppressed in a strong field. It was shown in I that if σ_{AL}, $(\Delta H, \theta, T)$ is considered as a function of θ for fixed values of T and $\Delta H = H - H_c$ (θ, T), then there is an angle θ_0 at which σ_{AL} has a maximum value, and θ_0 is not either 0° or 90°. While this is correct, the conclusion that this maximum in σ_{AL} is a characteristic of SPPL is in error. Conversely, it was found by later numerical calculations that the angular dependences of σ_{AL} for SPPL and ordinary superconductors are very similar.[22]

Recently the angular dependence of the fluctuation conductivity was measured by Aomine and Rinderer[18] for Al films in which $H_{c\parallel}$ is partly limited by Pauli paramagnetism. In their case the temperature was fixed only slightly below T_{c0}, and apparently the magnetic field was not strong enough to suppress σ_{MT} completely. Nevertheless they observed that σ_{fl} has a maximum at a field orientation which is close to, but not exactly parallel.

So far, however, there have been no experiments on σ_{fl} for superconductors definitely in the Pauli paramagnetic limit. One of the main purposes of the present communication is to report the result of such measurements for Al films. At the same time we theoretically reconsider the AL term. We also extend our consideration to the MT term in order to look for the characteristic behavior of SPPL. Another purpose is to clarify, both theoretically and experimentally, the effect of a perpendicular field on the fluctuation conductivity. In this case we assume that $H_{c\perp}$ is low enough so that Pauli paramagnetism is not important.

In Sec. II we discuss σ_{AL} in connection with the pair-breaking strength due to the magnetic field and show that for a given ratio of $H_{c\parallel}/H_{c\perp}$ one expects some universal behavior for σ_{AL} as a function of θ regardless of whether the samples are SPPL or ordinary superconductors. In Sec. III we consider the MT contribution in a magnetic field. Investigating the field dependence of the BCS vertex correction within the lowest-order approximation of KK[13] we show that the internal pair-breaking parameter δ_i (the part which was considered by KK) behaves in magnetic fields in a way very similar to σ_{MT} itself. δ_i is enhanced by a perpendicular field and is suppressed by a parallel field. In Sec. IV we describe our experimental measurements. The resistance of thin Al films was measured from 0.4 to 4.2 K and with magnetic fields up to 66 kOe. The angle between the plane of the film and the field could be varied from 0° to 90°. The films studied were less than 50 Å thick and had sheet resistances of a few hundred ohms per square. In Sec. V we discuss and summarize our findings.

II. ASLAMAZOV-LARKIN TERM

In this section we first review the results obtained in I and then reconsider their physical implications in order to make clear the effect of Pauli paramagnetism on superconducting fluctuations. It was shown in I that the AL contribution to the fluctuation conductivity, including the Pauli-paramagnetic effect, is given by

$$\sigma_{AL} = \frac{eT}{4\pi dD}\,\frac{F(\rho)}{H\sin\theta}\ , \tag{6}$$

with

$$F(\rho) = 2(\rho-1)\left[\psi\left(1+\tfrac{1}{2}\rho\right) - \psi\left(\tfrac{1}{2}+\tfrac{1}{2}\rho\right)\right] + 4/\rho - 2\ , \tag{7}$$

where

$$\rho = \frac{\epsilon_0^0(H,\theta) - \epsilon_0(T,H)}{2eHD\sin\theta} \tag{8}$$

and

$$\epsilon_0^n(H,\theta) = 2DeH(2n+1)\sin\theta$$

$$+(\tfrac{1}{3}D)(e\,dH\cos\theta)^2,\ n=0,\ 1,\ 2\ldots\ . \quad (9)$$

Furthermore $\epsilon_0(T, H)$ is determined by setting

$$P(\epsilon_0, H)=0\ , \quad (10)$$

where

$$P(\epsilon_0, H)\equiv\tau+\tfrac{1}{2}\left(1+\frac{b}{[b^2-(\mu_B H)^2]^{1/2}}\right)\psi(\tfrac{1}{2}+a_-)$$
$$+\tfrac{1}{2}\left(1-\frac{b}{[b^2-(\mu_B H)^2]^{1/2}}\right)\psi(\tfrac{1}{2}+a_+)-\psi(\tfrac{1}{2})\ , \quad (11)$$

with

$$a_\pm=\frac{1}{2\pi T}\left\{\tfrac{1}{2}\epsilon_0+b\pm[b^2-(\mu_B H)^2]^{1/2}\right\}\ .$$

Here $b=1/3\tau_{so}$ with τ_{so}^{-1} being the spin-orbit scattering rate of the conduction electrons, $D=\frac{1}{3}v_f l$ is the diffusion constant and ψ is the digamma function. For superconductors whose critical fields are limited entirely by the orbital motion of electrons Eqs. (10) and (11) give $\epsilon_0(T, H)=\epsilon_0^0(H_c, \theta)$, but for SPPL this is not the case. The use of Eqs. (8), (10), and (11) is a trick to take into account the Pauli paramagnetic effect. An alternative way to account for the effect of electron spin is to expand the pair propagator $\mathfrak{D}(n, \omega)$ from the beginning. If $b\ll 2\pi T$, we can write

$$[\mathfrak{D}(n, \omega)N(0)]^{-1}=P(-i\omega+\epsilon_0^n)\ ,$$
$$H\cong\tau+(\pi/8T)(-i\omega+\epsilon_0^n+\epsilon_p)\ , \quad (12)$$

where $\epsilon_p=0.54\mu_B^2H^2/T$. This expansion is only valid for relatively high temperatures $T\lesssim T_{c0}$, but the role of the Pauli paramagnetism is much clearer in Eq. (12). This propagator leads us in a straightforward manner to Eqs. (6)–(8), with ρ now given by

$$\rho=\frac{2De\sin\theta(H-H_c)+[\frac{1}{3}D(ed\cos\theta)^2+0.54\mu_B^2/T](H^2-H_c^2)}{2DeH\sin\theta}\ . \quad (13)$$

For $\Delta H\equiv H-H_c(\theta, T)\ll H$, we can approximate Eq. (13) by

$$\rho\simeq[1+eH_c(d^*\cos\theta)^2/(3\sin\theta)](\Delta H/H_c)\ , \quad (14a)$$

where d^* is defined by

$$(d^*\cos\theta)^2=(d\cos\theta)^2+1.62\mu_B^2/e^2DT\ . \quad (15)$$

If we set

$$F(\rho)=f(\rho)/\rho\ , \quad (16)$$

we can write Eqs. (6)–(11) as

$$\sigma_{AL}\cong\frac{e^2}{16d}\frac{f(\rho)T}{(\frac{1}{4}\pi De)[\sin\theta+(\frac{1}{3}e)H_c(d^*\cos\theta)^2]\Delta H}\ . \quad (17a)$$

Here $(\pi De/4)^{-1}$ is equal to the slope $\Delta H_{c\perp}/\Delta T$ of $H_{c\perp}$ versus T near T_{c0}. The function $f(\rho)$ is plotted in Fig. 1. So far we have been assuming that the temperature T is fixed and H is a variable. If H is fixed and T is varied, it is more convenient to write

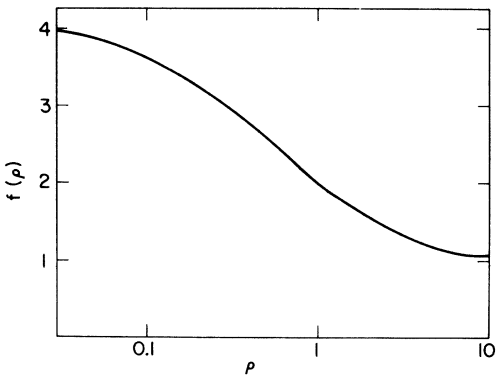

FIG. 1. $f(\rho)$ as a function of ρ. $f(\rho)$ is the enhancement factor of the AL term due to the perpendicular component of the magnetic field [see Eqs. (17a) and (17b)].

$$\rho=4[T-T_c(H, \theta)]/\pi DeH\sin\theta \quad (14b)$$

and

$$\sigma_{AL}=(e^2/16d)f(\rho)T/[T-T_c(H, \theta)]\ , \quad (17b)$$

where $T_c(H, \theta)$ is the transition temperature for the given field strength H and orientation θ.

One can see in Eqs. (12) and (9) that there are three terms which suppress superconductivity: the orbital terms due to the perpendicular and parallel components of the magnetic field and the spin term. There are no cross terms among these three terms. The last two terms are quadratic in H while the first is linear. The pair-breaking effect due to the Pauli spin is now expressed in the same form as that due to magnetic impurities,[23] or that due to orbital motion in the presence of a magnetic field. If $b\ll 2\pi T$, its pair-breaking strength does not depend on b near T_{c0}. At lower temperatures, where Eq. (12) is not valid, it is larger for smaller b. It is worth emphasizing that, if $H_{c\parallel}\gg H_{c\perp}$, $H_c(\theta, T)$ is not large enough for the quadratic terms to play an important role except for small θ, say, $\theta<5°$–$10°$, where the pair-breaking strength due to the perpendicular component is smaller. To be more precise, by solving Tinkham's formula we obtain

$$H_c(\theta)=(H_{c\perp}/\sin\theta)\left\{\tfrac{1}{2}+[\tfrac{1}{4}+(H_{c\perp}\cos\theta/H_{c\parallel}\sin\theta)^2]^{1/2}\right\}^{-1}$$
$$\approx H_{c\perp}/\sin\theta\ \text{ for }\theta\gtrsim 2\theta_t\ , \quad (18)$$

where θ_t is defined by

$$\theta_t=\cot^{-1}(H_{c\parallel}/2H_{c\perp})\ . \quad (19)$$

Physically, θ_t is the angle at which the pair-break-

ing regime changes from quadratic to linear.[24] Also we note in Eqs. (14a) and (17a) that for $\theta \gtrsim 2\theta_t$,

$$\sin\theta + \tfrac{1}{3} e H_c (d^* \cos\theta)^2 \simeq \sin\theta \quad , \tag{20}$$

which simply means that in this region of θ the parallel component of H is not important for σ_{f1}. It follows then that if the entire resistivity curve is plotted against the reduced field $H/H_c(\theta)$ for different T, the curve should be independent of θ for $\theta \gtrsim 2\theta_t$.

In Eq. (17) the Pauli paramagnetic effect is included by renormalizing the film thickness according to Eq. (15). Hence this effect is implicit if σ_{AL} is considered as a function of H. d^* does depend on θ; however, if $\theta_t \lesssim 10°$ (as is usually the case), a factor of $\cos^2\theta$ can be inserted into the last term in Eq. (15) and we can write

$$(d^*)^2 \approx d^2 + (1.62\,\mu_B^2)/(e^2 DT) \quad ,$$

where d^* is now independent of θ. It follows from this result that the effect of Pauli paramagnetism is also expressed almost completely implicitly for the case where σ_{AL} is considered a function of θ for a fixed ΔH. Figure 2 demonstrates this fact. σ_{AL} calculated from Eqs. (6)–(11) is plotted as a function of θ for a fixed ΔH for SPPL (curve A) and an ordinary superconductor (curve B). $H_{c\parallel}$ in curve A is limited almost entirely by Pauli paramagnetism while the $H_{c\parallel}$ of curve B is determined by the orbital motion. Curves A and B are normalized in such a way that they give the same values for $\theta = 90°$. One notes that except for the normalization factor, the field dependence of $\sigma_{AL}^{(A)}$ and $\sigma_{AL}^{(B)}$ are almost identical. It should also be pointed out that d^* is temperature dependent, and is larger for lower temperatures. This is in agreement with the observed temperature dependence of $H_{c\parallel}(T)$ in that $H_{c\parallel}$ for SPPL does not increase as much in going to lower temperatures as one would expect from the slope of $H_{c\parallel}^2$ against T near T_{c0}.

Finally we wish to discuss the physical significance of $f(\rho)$. As plotted in Fig. 1, $f(\rho)$ is a slowly varying function of ρ, which varies monotonically from a value of 4 for $\rho \ll 1$ to a value of 1 for $\rho \gg 1$. In the presence of a finite perpendicular component of the magnetic field $H\sin\theta$, the (orbital) energy levels of the fluctuating pairs are quantized as ϵ_0^n, $n = 0, 1, 2\ldots$ (Landau quantization). At each level there is a large degeneracy of states which otherwise would be distributed continuously between levels. In Eqs. (8) and (13) one sees that $\rho/2$ is the ratio of the excess $\epsilon^0 - \epsilon_{cr}$ of the pair-breaking strength above its critical value ϵ_{cr} to the energy spacing of the discrete levels. Here ϵ^n are the quantized energy levels which include the contribution from the spin

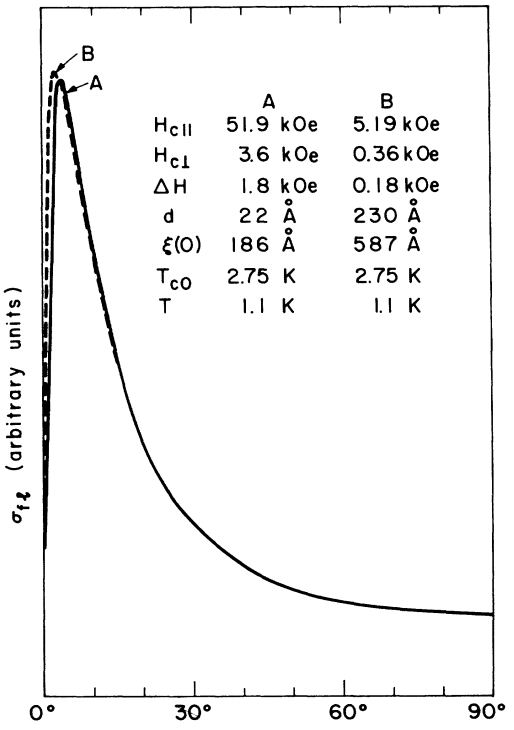

FIG. 2. Calculated angular dependence of σ_{f1} for fixed values of T and $\Delta H = H - H_c(\theta)$ for (A) SPPL and (B) an ordinary superconductor. The ratio $H_{c\parallel}/H_{c\perp}$ is assumed to be the same for both cases. Note the similarity of the shapes of the curves, especially that there are peaks for both cases.

$$\epsilon^n = \epsilon_0^n(H, \theta) + \epsilon_p(H) \quad , \quad n = 0, 1, \ldots$$

and

$$\epsilon_{cr} = \epsilon_0^0(H_c, \theta) + \epsilon_p(H_c) \quad .$$

with ϵ_p as defined after Eq. (12). Hence ρ gives a measure of how important the discreteness is, and $f(\rho)$ is the enhancement factor for the AL term due to the discreteness [see Eqs. (17a) and (17b)]. From Fig. 3 one can easily understand the reason why $f(\rho)$ for $\rho \ll 1$ is larger than $f(\rho)$ for $\rho \gg 1$. $\rho \ll 1$ means that the discreteness is important; in this case [see Fig. 3(a)], because of the Boltzmann factor, fluctuations which occur in the states of the lowest energy level ϵ^0 are larger than the sum of fluctuations which would occur at these levels if they were distributed continuously between ϵ^0 and ϵ^1 [see Fig. 3(c)], hence the AL term is enhanced by a perpendicular field in the vicinity of the transition point. (Whenever we talk about enhancement or suppression by a field, we mean enhancement or suppression after the shift of T_c, due to the field, is taken into account, unless otherwise stated.) For $\rho \gg 1$ [see Fig. 3(b)] it is obvious that the discreteness is not important, and $f(\rho) \approx 1$. The an-

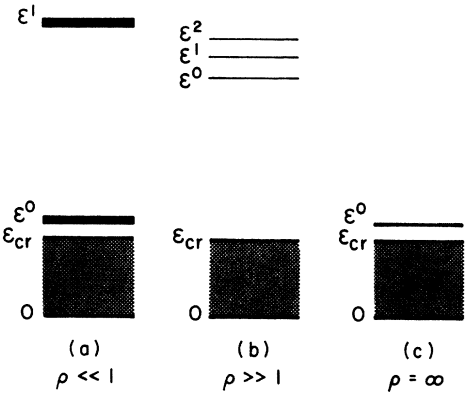

FIG. 3. Energy spectra of fluctuating pairs. This diagram illustrates the importance of the Landau quantization due to the perpendicular component of the magnetic field. ϵ^0 is the lowest energy level for the pairs; ϵ_{cr} is its critical value for superconductivity, that is, when $\epsilon^0=\epsilon_{cr}$ is satisfied, the superconducting transition occurs. ϵ^n, $n=1, 2\ldots$ are other Landau levels. If $\rho \ll 1$ [case (a)] (corresponding to $\epsilon^0-\epsilon_{cr}\ll\epsilon^0-\epsilon'$), more thermal fluctuations occur at the lowest energy states than in the case of continuous distribution [case (c)] of states, because of the large degeneracy at this level in the former case. For $\rho\gg1$ [case (b), the spectrum is almost a continuum and the discreteness is not important.

gular dependence of σ_{AL} shown in Fig. 1 is determined by two factors in Eq. (17a), namely, $f(\rho)$ and the quantity in the square bracket. If $f(\rho)$ is seen as a function of θ for a fixed ΔH such that $\Delta H \gg H_{c1}$, it increases very sharply from 1 for $\theta \simeq 0°$ to about 4 for $\theta \simeq 2\theta_t$ and then becomes approximately constant until $\theta = 90°$. From this fact and Eq. (20), we can see that σ_{AL} is smaller at both angular extremes, $\theta = 0°$ and 90° and has a maximum at some intermediate angle θ_0. θ_0 is approximately equal to θ_t, the angle at which the pair-breaking regime changes from being dominated by $H_{\|}$ or spin paramagnetism to the regime dominated by the perpendicular field. θ_0 is smaller for larger values of $a = H_{c\|}/H_{c1}$, and for $a > 100$, θ_0 is less than 1°.

III. MAKI-THOMPSON TERM

In this section we discuss the contribution from the Maki diagram (see Fig. 4) including the Pauli paramagnetic effect. Since the derivation of the MT term without including the Pauli paramagnetic effect is given in various places,[2,4,13,14] we shall only indicate how Pauli paramagnetism can be incorporated into σ_{MT}. The most important point is how the pair-breaking parameter is affected by Pauli paramagnetism. We calculate the pair-breaking parameter δ in a magnetic field within the lowest-order approximation of KK. For simplicity we set $b=0$. Since the MT term is important only in relatively weak fields, the pair propagator given by Eq. (12) is sufficient.

The one-particle Green's function for spinless electrons is given by

$$G(\omega, p) = (i\tilde{\omega} - \xi_p)^{-1} \ ,$$

where $\xi_p = v_f(p-p_f)$ and $\tilde{\omega} = \omega + (\frac{1}{2}\tau_e)\,\mathrm{sgn}\omega$ where τ_e is the electron mean free time. The Zeeman splitting can be included by replacing ω by $\omega + i\sigma\mu_B H$ provided that $\mathrm{sgn}(x)$ is interpreted as $\mathrm{sgn}(\mathrm{Re}x)$, where $\sigma = \pm 1$ is the spin of the electron under consideration. The vertex function $\Lambda_0(\omega_1, \omega_2)$, which includes corrections due to impurity scattering but not those due to Zeeman splitting or superconducting fluctuations, is given by

$$\Lambda_0(\omega_1, \omega_2) = |\tilde{\omega}_1 - \tilde{\omega}_2| \ (|\omega_1 - \omega_2| + Dq^2)^{-1} \ ,$$

where ω_1 and ω_2 are frequencies of the interacting electrons via the BCS interaction. It follows from the above considerations that the Zeeman splitting can be included in Λ_0 by replacing ω_1 and ω_2 by $\omega_1 + i\sigma\mu_B H$ and $\omega_2 - i\sigma\mu_B H$, respectively, where σ is the spin of the electron with frequency ω_1. Thus we obtain

$$\Lambda_0^{\sigma}(\omega_1, \omega_2) = \begin{cases} \dfrac{\tilde{\omega}_1 - \tilde{\omega}_2 + 2i\sigma\mu_B H}{\omega_1 - \omega_2 + 2i\sigma\mu_B H + Dq^2} & \text{for } \omega_1 > \omega_2 \ , \\ \Lambda_0^{-\sigma}(\omega_2, \omega_1) & \text{for } \omega_1 < \omega_2 \ . \end{cases} \tag{21}$$

The integral equation for the vertex function which includes the correction due to the pair fluctuations is shown diagrammatically in Fig. 5. By a careful examination one can convince oneself that the solution to this integral equation can be obtained by making the following replacements in the results obtained by KK:

$$\omega \to \omega + i\sigma\mu H, \quad \omega' \to \omega' - i\sigma\mu H \ ,$$
$$\Lambda_0 \to \Lambda_0^{\sigma}, \qquad K_0 \to \mathfrak{D}$$

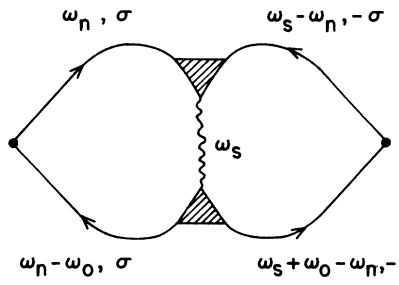

FIG. 4. Maki diagram. ω_s is the frequency of the fluctuations. In the text we consider only the case of $\omega_s = 0$. The wavy line is the pair propagator, and the triangular parts are vertex functions calculated in Fig. 5.

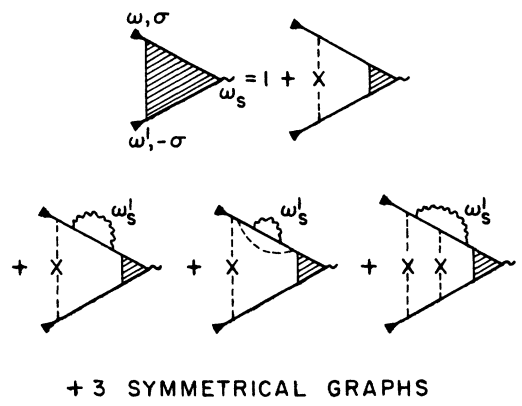

FIG. 5. Diagrammatic representation of the integral equation for the vertex function $\Lambda^{\sigma}(\omega, \omega')$; σ is the spin of the electron with frequency ω. Broken lines denote impurity scattering.

Hence the momentum-independent part of the vertex function is given for $\omega > 0$ and $\omega' < 0$ by

$$\Lambda^{\sigma}(\omega, \omega') = \frac{\tilde{\omega} - \tilde{\omega}' + 2i\mu_B \sigma H}{\omega - \omega' + 2i\mu_B \sigma H + Dq^2 + L^{\sigma}(\omega) + L^{-\sigma}(\omega')} \tag{22}$$

and

$$L^{\sigma}(\omega) = \frac{8T^2}{N(0)\pi} \frac{eH\sin\theta}{\pi d} \times \sum_m [(\epsilon + \epsilon^m)(2\omega + 2i\mu_B \sigma H + 2\epsilon_0^m + \epsilon)]^{-1} ,$$

with $\epsilon = (8T/\pi)\tau$. For $\omega < 0$ and $\omega' > 0$,

$$\Lambda^{\sigma}(\omega, \omega') = \Lambda^{-\sigma}(\omega', \omega), \quad L^{\sigma}(\omega) = L^{-\sigma}(|\omega|) .$$

The extra conductivity due to the Maki diagram is given by

$$\sigma_{MT} = \lim_{\omega_0 \to 0} \frac{1}{\omega_0} [Q^M(\omega_0) - Q^M(0)], \tag{23}$$

where

$$Q^M(\omega_0) = 2\pi e^2 DTN(0) \sum_m P(m, \omega_0) \mathfrak{D}(m, 0) \tag{24}$$

and

$$P(m, \omega_0) = T\,\mathrm{Re} \sum_{0 < \omega_n < \omega_0} [\omega_n + \tfrac{1}{2}\epsilon_0^m + i\mu_B H + L^{+}(\omega_n)]^{-1} \times [\omega_0 - \omega_n + \tfrac{1}{2}\epsilon_0^m - i\mu_B H + L^{-}(\omega_0 - \omega_n)]^{-1} . \tag{25}$$

We replace $L^{\sigma}(\omega)$ by its value for $\omega = 0$. Summing over n and then m in Eqs. (25) and (24), respectively, and substituting the resulting expression for Q^M into Eq. (23) we obtain

$$\sigma_{MT} = (e^2/8d)(\tau' - \delta)^{-1} [\psi(\tau'/\eta) - \psi(\delta/\eta)] , \tag{26}$$

where $\eta = (\pi/2T)\, DeH\sin\theta$,

$$\tau' = \tau + (\pi/8T)\epsilon^0 \cong \ln[T/T_c(H, \theta)] ,$$

and

$$\delta(H, \theta) = \delta_i(H, \theta) + \delta_e(H, \theta) , \tag{27}$$

with

$$\delta_e(H, \theta) = (\pi/8T)\epsilon_0^0(H, \theta) \tag{28}$$

and

$$\delta_i(H, \theta) = (\pi/4T)\,\mathrm{Re}\, L^{+} . \tag{29}$$

The pair-breaking function L^{σ} is given by

$$L^{\sigma} = A[\tau' - (\pi/8T)(\epsilon_0^0 + 2i\sigma\mu_B H)]^{-1} \times [\psi(\tau'/\eta) - \psi(\delta_L/\eta)] , \tag{30}$$

where $A = T/4N(0)\pi dD$ and

$$\delta_L = (\pi/16T)(\epsilon_0^0 + 2i\mu_B H) + \tfrac{1}{2}\tau' . \tag{31}$$

For $\theta = 0$ or $H = 0$, Eqs. (26) and (30) are undefined and must be replaced, respectively, by

$$\sigma_{MT} = (e^2/8d)(\tau' - \delta)^{-1} \ln(\tau'/\delta) \tag{32}$$

and

$$L^{\sigma} = A[\tau' - (\pi/8T)(\epsilon_0^0 + 2i\sigma\mu_B H)]^{-1} \ln(\tau'/\delta_L) . \tag{33}$$

For $H = 0$ these expressions reduce to the corresponding ones obtained by KK.

A few comments are in order. First, Pauli paramagnetism does not contribute to the external pair-breaking parameter δ_e. If it did, we would have $\epsilon_0^0 + 2i\mu H$ instead of ϵ_0^0 on the right-hand side of Eq. (28). A cancellation of the $i\mu_B H$ terms occurred because these terms come in with opposite sign in the two different factors in Eq. (25). These factors originate from the denominators of the vertex functions $\Lambda^{\sigma}(\omega_0 - \omega_n)$ and $\Lambda^{\sigma}(\omega_n - \omega_0, \omega_0 - \omega_n)$ at each of the pair-propagator vertices in the Maki diagram. Since we are considering the anomalous contribution $[\omega_n(\omega_n - \omega_0) < 0]$, the signs of $i\mu_B H$ in these vertex functions are opposite. Second, the pair-breaking function L^{σ} is very similar to σ_{MT}. The similarity becomes clearer if we write

$$\tau' - (\pi/8T)(\epsilon_0^0 + 2i\mu_B H) = 2(\tau' - \delta_L)$$

in Eqs. (30) and (33). There is, however, an essential difference. Each of the last three diagrams in Fig. 5 contains two vertex functions $\Lambda_0^{\sigma}(\omega, \omega_{s'} - \omega)$, where $\omega_{s'}$ is the frequency of the pair propagator. The signs of $i\mu_B H$ in these vertex functions are the same; hence no cancellation of $i\mu_B H$ occurs, and $2i\mu_B H$ is present in δ_L. This term suppresses L^{σ} in a parallel magnetic field.

Let us first consider the case of perpendicular fields. If $eD/\mu_B \gg 1$, the term $2i\mu_B H$ can be ignored in Eq. (31), and

$$\delta_L \approx (\pi/16T)2DeH + \tfrac{1}{2}\tau' = \tfrac{1}{2}(\delta_e + \tau') .$$

From the similarity of δ_L to δ, and L^{σ} to σ_{MT} one

can easily see that a perpendicular field increases L^{σ} because of the Landau quantization. If δ_i were unaffected by a field (as in the Thompson theory[4]), the Landau quantization would enhance σ_{MT} for the reason discussed in Sec. II. Thus a perpendicular field gives two competing effects on σ_{MT}: the suppression of fluctuations due to the increase of δ_i and the enchancement of fluctuations due to the Landau quantization. By numerical calculations it appears that the over-all effect is the suppression of σ_{MT} for most cases.

For $\theta = 0$ (parallel field case) if the film is sufficiently thick,

$$\delta(H) \approx \delta_e(H) \gg \delta(0)$$

and σ_{MT} is suppressed by a parallel field. On the other hand, if Dd^2 is very small and $H_{c\parallel}$ is limited by Pauli paramagnetism, $\delta_e \approx 0$ and δ_i is the leading contribution to δ in Eq. (27). Now L^{σ} (and therefore δ_i) is suppressed by a parallel field because of the term $2i\mu_B H$ in δ_L. Hence we expect that σ_{MT} for SPPL is enhanced by a parallel field. However, in practice Dd^2 is finite and for a strong enough field, δ_e becomes large, and σ_{MT} is suppressed.

The approximation which we have used may be too naive. In fact KK found that in order to obtain agreement with experiment it is necessary, first to take into account the frequency dependence of the pair-breaking function L, which we have neglected, and second to sum over the frequency of fluctuations. Nevertheless, we believe that the above conclusions are essentially correct, independent of the approximations made, since they originate from the fundamental properties of the diagrams. These conclusions are that L^{σ} is increased by a perpendicular field and that σ_{MT} for a SPPL is enhanced by a parallel field.

IV. EXPERIMENTAL METHODS AND RESULTS

A. Experimental technique

The Al films used in this study were formed by evaporation on liquid-nitrogen-cooled glass substrates in a vacuum of 10^{-6} Torr. The film thickness was determined using a quartz-crystal oscillator. To avoid edge effects, the films were photoetched to form the pattern shown in Fig. 6. The samples were immersed in liquid He^3 or He^4 depending on the temperature range to be studied. High-field measurements were made using a transverse-access Bitter solenoid with a maximum field of 66 kOe. Here, the entire cryostat could be rotated to obtain the desired angle between the field direction and the plane of the sample. Some low-field measurements were made in a conventional iron magnet which could be rotated to adjust the field angle.

The data were obtained in a conventional dc way, with a constant current through the sample giving rise to a voltage proportional to the sample resistance R. Most of the high-field, low-temperature data were in the form of x-y recorder plots of R vs T or H. The high-temperature low-field data were obtained from the printed output of a digital voltmeter. Checks were made for possible thermal voltages or current drift.

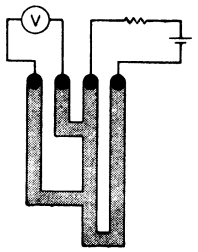

FIG. 6. Diagram showing sample shape. The width of the photoetched lines is 0.8 mm.

The problem of determining the normal resistance is a troublesome one. At low temperature and high parallel field, R becomes independent of H at constant T for $H > H_{c\parallel}$. In this region, fluctuations are suppressed because of the first-order phase transition in SPPL films. Therefore, this H-independent value of R was chosen to be R_n. Some of the films, however, were not studied at low T, so this method could not be used. For these films R_n was obtained by extrapolating to $H = 0$ the value of R vs $H_\perp$ for $H_\perp \gg H_{c\perp}$. This method was used rather than the conventional method of plotting $1/R$ vs $1/H_\perp$ and extrapolating to $1/H_\perp \to 0$ because the films had a negative magnetoresistance at high fields. This effect will be discussed in Sec. V.

The film thickness was measured during evaporation by the frequency change of a quartz crystal oscillator. The thickness of the films after evaporation (d_0 in Table I) was about 32 Å. The films were then warmed to room temperature, exposed to the laboratory atmosphere for a few minutes, coated with photoresist, exposed with the circuit pattern, developed, and etched. Solder terminals were applied and the films were mounted in the Dewar and measured. Before measurement the total exposure to the laboratory atmosphere was about 2 h. The oxide layer formed on Al films under these conditions is estimated from the resistance of tunnel barriers and from previous measurements[25,26] to be 15–20 Å. The thickness of the oxide film is known to be about 1.4 times thicker than the Al film which it replaces.[26] Thus the estimated decrease in Al-film thickness caused by oxidation is estimated to be 11–14 Å. The values for the corrected thickness d given in Table I were found in this way.

An additional check on the film was obtained by

TABLE I. Properties of Al films.

Film No.	Thickness determinations[a] d_0(Å)	d(Å)	d' (Å)	$R_\square$ (Ω)	T_{c0}(K)	$\xi(0)$ (Å)	$H_{c\parallel}(0)$ (kOe)	$H_{c\perp}$(kOe)
Al−1	34	20–30		185	2.22	256	45.7	3.3
Al−2			24	333	2.68	168	51.9	4.4
Al−3	32	18–21	23	426	2.49	270		
Al−4	29	15–18	22	510	2.49	161	49.0	

[a] d_0 is the thickness determined from the crystal monitor, d is obtained by substracting an estimated oxide thickness from d_0, and d' is derived from comparison of R with measurements on other films of R vs d_0 during evaporation.

comparing the resistance of the present films after oxidation with the resistance of similar films during evaporation on a cooled substrate. The resistance-derived thickness d' is also given in Table I.

B. Angular dependence of σ_{f1}

In this subsection we consider the angular dependence of σ_{f1}. Since the measurements were taken at low temperature $T \ll T_{c0}$, the critical field H_c should be high enough to suppress the MT contribution, and according to theory we should analyze our data entirely on the basis of the AL contribution, that is, $\sigma_{f1}^{th} = \sigma_{AL}$. Figure 7 shows the resistivity R as a function of the magnetic field for a fixed temperature $T = 0.2\ T_{c0}$ for various angles θ. H is scaled according to $H_c(0)$. Note that in these plots, we have identical curves for $\theta \geq 25°$ ($\equiv 2\theta_t^{expt}$) as should be the case. This value compares with the theoretical one $2\theta_t^{th} = 16°$ obtained from Eq. (19). We also observed that the functional relation of Eq. (18) is satisfied experimentally. From these we conclude that if $H_{c\parallel}/H_{c\perp} \gg 1$, both H_c and σ_{f1} are limited by the perpendicular component $H\sin\theta$ of H alone for a large range of θ: $\theta_t \leq \theta \leq 90°$. In Fig. 8 we plot $\tilde{\sigma}_{f1}^{-1} \equiv \sigma_n/\sigma_{f1}$ as a function of H (without scaling) for various values of θ. Determination of the normal conductivity was relatively easy because of the absence of the MT contribution. For a large enough field $H \gg H_c$, the resistivity R was observed to be independent of H. In this plot, the smaller the slope, the larger the extra conductivity σ_{f1}. One notes that the transition is sharper for both $\theta = 0°$ and 90° and is less sharp for intermediate angles. σ_{f1} has a maximum at $\theta \approx 14.7°$ (the slope has a minimum as a function of θ for a given value of $\tilde{\sigma}_{f1}^{-1}$). A comparison of these data with Eqs. (6)–(11) is done in Fig. 9 where we plot $(\tilde{\sigma}_{f1})^{-1}$ for selected values of θ. First we observe that the experimental curves are much flatter than the theory predicts near the transition point. This makes a systematic determination of $H_{c\perp}$ and $H_{c\parallel}$ difficult. From Fig. 8 we chose $H_{c\perp}$ and $H_{c\parallel}$ to be 4.4 and 51.9 kOe, respectively. These values determine D and d by the use of Eqs. (10) and (11) for an assumed value of b. We set $b = 0.2\Delta$, which was obtained by theoretically fitting $H_{c\parallel}(T)$ in an earlier experiment for similar films.[27] Here Δ is the superconducting energy gap in zero temperature and zero field. Theoretical values for $H_c(\theta)$ can now be determined for all θ again from Eqs. (10) and (11). The experimental point at each $\Delta H \equiv H - H_c(\theta)$ was obtained from Fig. 8 for the corresponding H and θ, that is, no arbitrary adjustments were made for $H_c(\theta)$ at each angle. If b/Δ were assumed to be 0.5, we would obtain a slightly larger value for d, but $H_c(\theta)$ as well as σ_{f1}^{th} would be almost unchanged. The theoretical curves are bent upward; this tendency is most obvious for $\theta = 2.7°$. As one sees from the approximate expression Eq. (17a), $(\sigma_{f1}^{th})^{-1}$ vs ΔH should be linear if $f(\rho)$ were constant. However, with increasing ΔH, ρ increases and $f(\rho)$ decreases, meaning that the Landau quantization is less important for larger ΔH. Consequently $\tilde{\sigma}_{f1}^{-1}$ vs ΔH curves bend upward. The experimental curves have this character, although the slopes for smaller ΔH are much smaller than the theory predicts; as ΔH increases, the slopes of $(\tilde{\sigma}_{f1}^{expt})^{-1}$ vs ΔH approach the theoretical values. If the MT contribution were important these curves would bend downward, but there is no indication of this effect in the measured curves. Comparison between theory and experiment for $\tilde{\sigma}_{f1}(\theta)$ as a function of θ for a given ΔH (the type of plot shown in Fig. 2) would be interesting. However, the result of such an

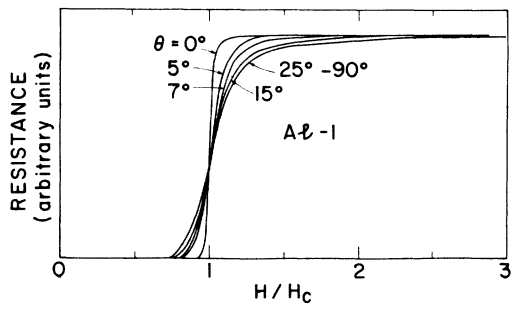

FIG. 7. Resistivity R as a function of the scaled magnetic field $H/H_c(\theta)$ for Al−1 with $T = 0.44$. Note for $\theta \geq 25°$, curves are independent of θ.

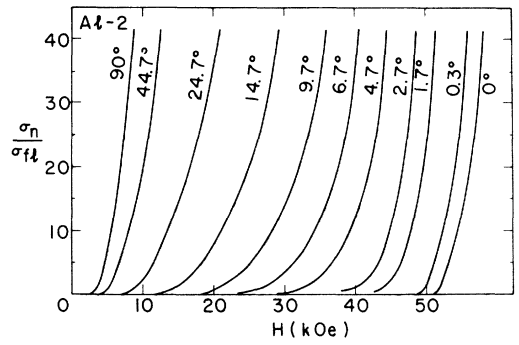

FIG. 8. Experimental curves for σ_n/σ_{f1} as a function of H for various values of the angle θ with $T=1.15$. The transition is broader (larger σ_{f1}) for $\theta=4.7°$ to 14.7° and sharper at both ends, $\theta=0°$ and 90°.

analysis of the experimental data is strongly affected by the choice of $H_{c\perp}$ and $H_{c\parallel}$, because for example, if we had chosen smaller values for $H_{c\perp}$ and $H_{c\parallel}$, all the experimental curves shown in Fig. 9 would have been shifted to the right. Hence such an analysis is not suitable for the present case. Instead, if we compare the slope of $(\tilde{\sigma}_{f1}^{\text{expt}})^{-1}$ and $(\tilde{\sigma}_{f1}^{\text{th}})^{-1}$ at a certain value of $(\tilde{\sigma}_{f1})^{-1}$, the result should be unaffected by the choice of $H_{c\perp}$ and $H_{c\parallel}$. Such plots are shown in Fig. 10. Curves A and A' are the field derivatives of $(\tilde{\sigma}_{f1}^{\text{expt}})^{-1}$ and $(\tilde{\sigma}_{f1}^{\text{th}})^{-1}$, respectively, taken at $\tilde{\sigma}_{f1}^{-1}=35$, and curves B and B' are those at $\sigma_{f1}^{-1}=7$. While the minimum of curve A is at about 20° and that of A' at 8°, general agreement is not bad. Also the shapes of curves B and B' are similar, although curve B lies appreciably

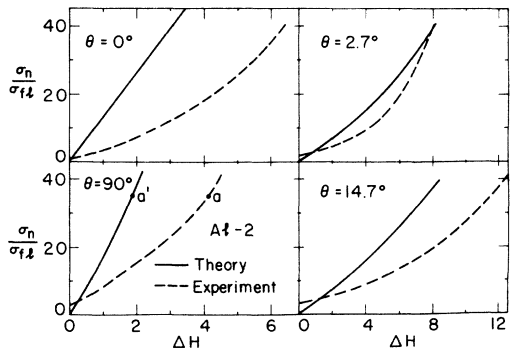

FIG. 9. Comparison between theoretical (solid-line) and experimental (dashed-line) curves of σ_n/σ_{f1} as functions of ΔH for $\theta=0°$, 4.7°, 14.7°, and 90°. Experimental curves are the same as in Fig. 8. For smaller ΔH, experimentally observed σ_{f1} are larger than theoretical values. However, with increasing ΔH, the slopes of the experimental curves increase. For larger ΔH they are comparable with those of corresponding theoretical values. For points a and a' see the caption of Fig. 10.

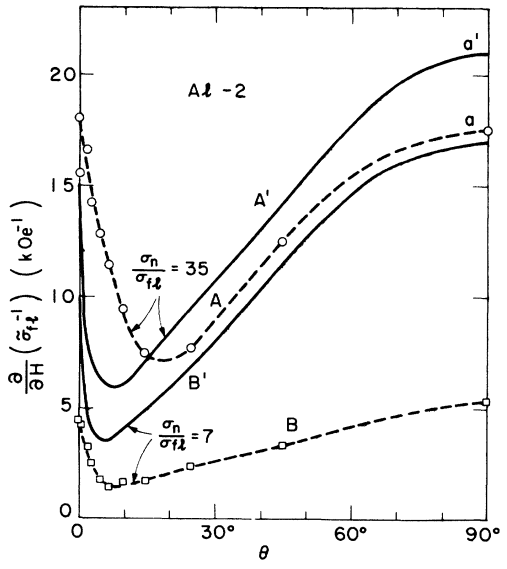

FIG. 10. Field derivatives of σ_n/σ_{f1} as a function of θ. Dashed curves A' and B' are corresponding experimental values taken at $(\sigma_n/\sigma_{f1})=35$ and 7, respectively. Solid curves A' and B' are corresponding theoretical values. For example, points a and a' in this figure represent the slopes of the curves in Fig. 9, at points marked a and a', respectively.

lower than B'. If curve B is expanded by a factor of 3 in the vertical direction, curves B and B' are in quite good agreement. We shall come back to this point in Sec. V.

C. σ_{fl} near T_{c0}

In this subsection we analyze our data of σ_{f1} near T_{c0}. In Fig. 11 we plot $\tilde{\sigma}_{f1}^{-1}$ as a function of the temperature with and without a magnetic field. A is the AL slope $\tilde{\sigma}_{\text{AL}}^{-1}=(1.52\times10^{-5}R_{\square})^{-1}\tau$ for zero field. Experimental points for $H=0$ follow this slope in the neighborhood of T_{c0}. However, near $T=2.7$ °K and above they tend to deviate from it. This effect is attributable to the additional contribution from the MT term. The dashed curve (B) indicates the theoretical values of $(\tilde{\sigma}_{\text{MT}}+\tilde{\sigma}_{\text{AL}})^{-1}$, where $\tilde{\sigma}_{\text{MT}}$ is obtained from Eqs. (3) and (4). Curve B falls below the experimental points, and apparently the empirical formula Eq. (4) does not hold for the present case. Keller and Korenman obtained Eq. (5) from Eqs. (29) and (33) by using the relation

$$[N(0)\,dD]^{-1}=4.86\times10^{-4}R_{\square}\ . \tag{34}$$

If we apply this relation for the present sample, calculated values of $(\tilde{\sigma}_{\text{MT}}+\tilde{\sigma}_{\text{AL}})^{-1}$ fall below the dashed line.

With a perpendicular field of 1165 Oe, T_c is shifted from 2.52 to 1.94 K. In choosing the values of T_c we have extrapolated the linear portion

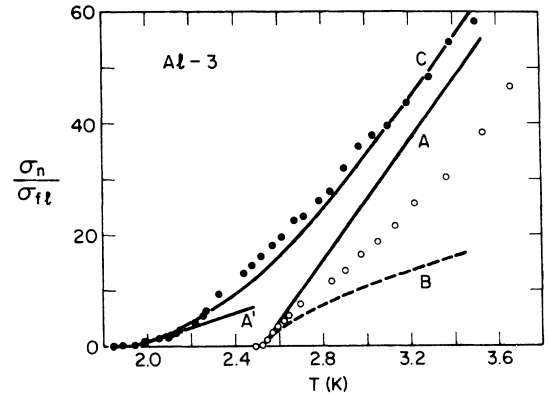

FIG. 11. σ_n/σ_{fl} vs T for $H=0$ (open circles) and for $H_\perp=1165$ Oe (solid circles). Curve A is the AL prediction for σ_n/σ_{fl} in zero field while B represents the sum of the AL and MT contributions using the empirical value for δ. Curve C was calculated from the AL theory for a perpendicular field. Curve A' has a slope equal to $\frac{1}{4}$ that of A. Experimental points with zero field follow A near T_{c0} and then deviate from it because of the MT contribution. The deviation, however, is not as large as Eqs. (3) and (4) predict. Note that the MT term is enhanced by a parallel field. With a perpendicular field, the AL contribution is enhanced near T_c, and the MT contribution is suppressed.

of σ_n/σ_{fl} to zero disregarding a very small resistance tail corresponding to the last point or two. This tail is probably caused by sample inhomogeniety. The theoretical curve C was obtained from Eqs. (6)–(11) (AL contribution) and can be approximated by Eq. (14b). In the vicinity of T_c, the slope of C is according to theory equal to $\frac{1}{4}$ of the slope of A and is shown by A'. A' fits the experimental data satisfactorily in this region near T_c. Well above T_{c0} the theoretical curve C becomes parallel to A and fits the experimental data reasonably well. This result shows that the MT contribution is almost completely suppressed by the field. The coherence length $\xi(0)$ was determined from the shift of T_c by the perpendicular field.

In Fig. 12, we show measurements of $\sigma_n/\sigma_{fl} = \tilde{\sigma}_{fl}^{-1}$ as a function of T for various values of parallel magnetic field H. The MT contribution appears to be suppressed more strongly as the field is increased. However, $\tilde{\sigma}_{fl}^{-1}$ does not approach the value predicted by the AL theory, except perhaps very near T_c. In high fields, the slopes of the curves decrease at high temperatures. At the highest fields (not shown), $\tilde{\sigma}_{fl}^{-1}$ has a negative slope. This behavior is related to the maximum in the second-order phase transition (part of which is a supercooling curve) of SPPL. This behavior was observed by Tedrow, Meservey, and Schwartz[20] and analyzed by Fulde and Maki.[16] No enhancement of the MT contribution by a parallel field was observed.

V. DISCUSSION

A. Determination of normal resistance

As mentioned in Sec. IV the conventional method to determine R_n by plotting $1/R$ vs $1/H_\perp$ for $T \simeq T_c$ and extrapolating to $1/H_\perp \to 0$ was not useful. In fact our films showed a resistance maximum at fairly low fields (15 kOe). The field dependence of R for $H_\perp$ well above $H_{c\perp}$ ($T \simeq T_{c0}$) appeared to be linear. Therefore, to obtain R_n, we extrapolated this linear portion back to $H_\perp = 0$ and the intercept with the $H_\perp = 0$ axis we took to be R_n (see Fig. 13). This method assumes that σ_{fl} is very small for $H_\perp \gg H_{c\perp}$. The value of R_n for sample Al-4 by this method was about 0.3% larger than that at the maximum of the R vs $H_\perp$ curve. The explanation of this negative magnetoresistance is not yet known, but it is the magnetic field normal to the film plane which causes the effect. As mentioned previously for those films for which $H_{c\parallel}$ was measured at low temperatures the normal resistance at high parallel fields was used to determine R_n.

B. Angular dependence of σ_{fl}

Theory and experiment are qualitatively in agreement concerning the angular dependence of σ_{fl}.

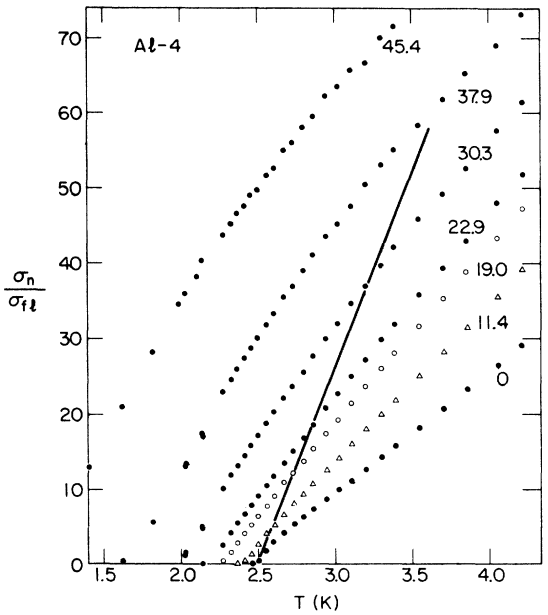

FIG. 12. σ_n/σ_{fl} as a function of T for various parallel magnetic fields, listed on the figure in kOe. The solid line shows the prediction of the AL theory. That the slope of the data increases with increasing field indicates that for this sample σ_{MT} is suppressed rather than enhanced by the field.

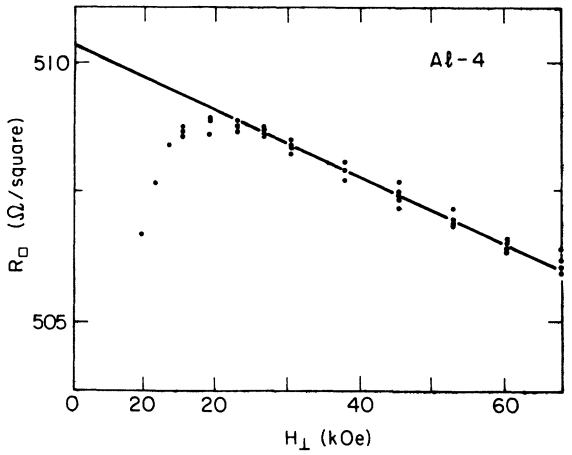

FIG. 13. Construction used to find R_n for films Al−3 and Al−4. The high-field portion of the plot of R vs $H_\perp$ is extrapolated back linearly to $H_\perp = 0$. The intercept with the R axis is chosen to be R_n.

There is an angle θ_0 of the maximum $\sigma_{f1}(\theta)$ near $\theta = 0°$; this fact is strong evidence for the quantization of the energy spectrum of the fluctuation modes due to the perpendicular component of the magnetic field. This result should be compared with a recent specific-heat measurement.[28] It has been found that because of the Landau quantization, the extra specific heat due to fluctuations for a bulk superconductor behaves in a strong magnetic field like that of a one-dimensional superconductor.[28]

A quantitative discrepancy in the low-temperature and high-field region is that in the neighborhood of H_c, σ_{f1}^{expt} is larger by some factor for all θ than the theoretical value. Since this is true even for the parallel field case, it cannot be due to flux-flow resistivity. Similar roundings in the critical region in the zero field were investigated by Chien and Glover[29] and were found to be closely related to the scattering by the film-substrate boundary. In the present case, too, the rounding may be caused by surface scattering. And the fact that the rounding is much larger for our case (particularly for a strong magnetic field) may be because the film is much thinner and surface scattering is playing a more important role.

On the other hand, the rounding in the critical region might be caused by inhomogeneity of the films. A spatial variation of thickness or mean free path would lead to a spatial variation of critical field. If for some position $\vec{r}$, $H_c(\theta, \vec{r})$ is larger than its average $H_c(\theta)_{av}$, it is so for all θ at that value of $\vec{r}$. It follows that the observed σ_{f1}^{expt} at $H = H_c(\theta)_{av}$, for example, will contain the extra conductivity of the fraction which is superconducting at that field (and this fraction is the same for all θ). Since σ_{AL}^{1} is roughly linear in ΔH, we expect the dependence of $[\partial(\sigma_{f1}^{expt})^{-1}/\partial H]_{H=H_c(\theta)_{av}}$ to be approximately the same as that of a homogeneous film except for a constant factor (which accounts for the fact that a fraction of the film is still superconducting). For H greater than the maximum value of $H_c(\theta, r)$ we expect the slope $\partial(\sigma_{f1}^{expt})^{-1}/\partial H$ to be relatively unaffected by the inhomogeniety because the entire film is now in the normal state. This explanation may account for the anomalously large value of σ_{f1}^{expt} and the fact that qualitatively it agrees with theory. If the inhomogeneity does not change T_{c0} much, it should not cause a broadening of the transition in zero field (in agreement with our results shown in Fig. 11).

C. σ_{f1} near T_{c0}

The purpose of taking data near T_{c0} was (i) to see if the AL contribution to σ_{f1} is enhanced by a perpendicular field in the neighborhood of the transition as predicted by Eqs. (14b) and (17b) (note $f(\rho) = 4$ for $\rho \ll 1$) and (ii) to find how the MT term behaves in zero and weak magnetic fields. Concerning the first point we observed that σ_{f1}^{expt} is enhanced about as much as the theory predicts. To check if this enhangement is anomalous (similar to that found at lower temperatures) we took the measurements with a parallel field $H_\parallel = 30$ kOe (for which $T_c = 2.0$ K). In this case the result was only a shift of T_c and no enhancement of σ_{f1} was observed except for the immediate neighborhood of T_c. That the observed enhancement with the perpendicular field was not quite as large as the theory predicts might be attributed to the adverse effect of the grain boundaries in the film on Landau quantization, since the radius of the Landau orbits is much larger than the average grain size. Despite this discrepancy, however, we conclude that the observed enhancement of the AL contribution is further evidence of the quantization of the energy levels of the fluctuating pairs. Since this property is not a characteristic of SPPL the experiment could have been done on thicker and cleaner films, but the films used were useful in that they excluded the MT contribution. The present result contrasts with that of Aomine and Rinderer who found that the perpendicular field does not enhance the fluctuation conductivity more than 20% of the zero-field value.[12] The latter may be because of the decreased mean free path caused by using an oxygen atmosphere in evaporation. It is probable that this procedure increases the oxide in the grain boundaries and would be very effective in suppressing Landau quantization effects.

Concerning the second point, we found that at zero field the MT contribution was less than what the empirical formulas Eqs. (3) and (4) predict. Equations (3) and (5) also predict values larger than

those measured. In the latter case if we sum up the effect of fluctuations of finite frequencies, the agreement will improve. Keller and Korenman found that this summation is more important for dirtier samples. In this respect our theoretical treatment of the MT term is incomplete for application to dirty superconductors. At the same time since the normal-state conductivity is a sensitive quantity, Eq. (34) may not be reliable for thin disordered films such as ours. Apparently the suppression of the MT term in disordered films is a universal phenomenon. It is still an open question whether the suppression arises entirely from the higher-order corrections due to fluctuations or that there are other mechanisms for it. If the former supposition is correct we can expect that our theoretical conclusions concerning the magnetic field behavior of the MT term should be at least qualitatively correct. This conclusion is based on the validity of the cancellation of the $i\mu H$ term discussed in Sec. III for fluctuations of finite frequencies. Our failure to observe enhancement of σ_{MT} in a parallel field could simply be caused by not having films with small enough values of d^2D.

VI. CONCLUSIONS

Theoretically we have obtained the following results. (i) Although Pauli paramagnetism is important in σ_{AL}, its effect can be included by renormalizing the thickness of the film, and therefore it is implicit in σ_{AL}. (ii) The fact that $\sigma_{AL}(\Delta H, \theta, T)$ has a maximum at some angle $\theta_0 \neq 0$, 90° for given values of ΔH, and T is a consequence of the Landau quantization of the paired electron orbits. (iii) A perpendicular field enhances σ_{AL} and suppresses σ_{MT}. (iv) In SPPL, σ_{MT} is enhanced by a weak parallel field.

Experimentally we have made the following observations (i) The angular dependence of σ_{AL} is in satisfactory agreement with the theory and, in particular, there exists an angle θ_0 for which the fluctuations are a maximum. (ii) The σ_{AL} is enhanced roughly by a factor of 4 by a perpendicular field. (iii) σ_{MT} appears to be suppressed by a perpendicular field. (iv) σ_{MT} in SPPL was not observed to be enhanced by a weak parallel field. Observations (iii) and (iv), are not in quantitative agreement with theory.

ACKNOWLEDGMENTS

We wish to thank P. Fulde for useful discussions and suggestions, and T. Aomine, R. Hake, J. Keller, and V. Korenman for useful and informative discussions. Correspondence with R. E. Glover, III is also gratefully acknowledged. We wish to acknowledge the help of R. MacNabb in preparing the films and of M Blaho in making the measurements.

---

*Present address: Institut für Theoretische Physik, Freie Universität Berlin 33, Arnimallee 3, W. Berlin. A part of this work was carried out at the present address.

†Supported by the National Science Foundation.

[1]L. G. Aslamazov and A. I. Larken, Phys. Lett. A 26, 238 (1968); Fiz. Tverd. Tela 10, 1104 (1968), [Sov. Phys.-Solid State 10, 875 (1968)].

[2]K. Maki, Prog. Theor. Phys., 40, 193 (1968).

[3]R. E. Glover, III, Phys. Lett. A 25, 542 (1967).

[4]R. S. Thompson, Phys. Rev. B 1, 327 (1970); in *Proceedings of the International Conference on the Science of Superconductivity*, edited by F. Chilton (North-Holland, Amsterdam, 1971), p. 296.

[5]A. Schmid, Phys. Kondens. Mater. 5, 302 (1966); E. Abrahams and J. W. F. Woo, Phys. Lett. A 27, 117 (1968).

[6]H. Schmidt, Z. Phys. 216, 336 (1968); H. J. Mikeska and H. Schmidt, Z. Phys. 230, 239 (1970).

[7]P. Fulde and K. Maki, Phys. Kondens. Mater. 8, 371 (1969); K. D. Usadel, Z. Phys. 227, 260 (1969); G. E. Clarke and D. R. Tilley, J. Phys. C 3, 2448 (1970); K. Maki and H. Takayama, Prog. Theor. Phys. 46, 1651 (1971).

[8]W. E. Masker, S. Marčelja, and R. D. Parks, Phys. Rev. 188, 745 (1969). W. E. Masker and R. D. Parks, Phys. Rev. B 1, 2164 (1970); M. Strongin, O. F. Kammerer, J. Crow, R. S. Thompson, and H. L. Fine, Phys. Rev. Lett. 20, 922 (1968).

[9]J. E. Crow, R. S. Thompson, M. A. Klenin, and A. K. Bhatnagar, Phys. Rev. Lett. 24, 371 (1970).

[10]S. Danner and F. Baumann, Phys. Lett. A 33, 83 (1970). In this reference, the authors compare their experimental data with the AL contribution, assuming that a perpendicular field enhances the AL contribution by a factor of 4, and obtained an agreement within 2.5%. However, as can be seen in our Eqs. (13) and (17a) and Fig. 1, the enhancement factor $f(\rho=1)$ is not 4 but 2 for $H \gg H_{c1}$, which essentially is the region they investigated. Furthermore, experimentally the enhancement factor should be determined relative to the observed zero-field (temperature-dependent) fluctuation conductivity because in many cases the experimental zero-field AL contribution is larger than the theoretical one. The observed fluctuation conductivity in this reference may be due to both AL and MT contributions.

[11]K. Kajimura and N. Mikoshiba, J. Low Temp. Phys. 4, 331 (1971).

[12]T. Aomine and L. Rinderer, J. Low. Temp. Phys. 6, 323 (1972).

[13]J. Keller and V. Korenman, Phys. Rev. Lett. 27, 1270 (1971); Phys. Rev. B 5, 4367 (1972).

[14]B. R. Patton, Phys. Rev. Lett. 27, 1273 (1971).

[15]M. A. Klenin and J. Crow (unpublished); M. A. Klenin, Ph.D. thesis (University of Pennsylvania, 1970) (unpublished).

[16]P. Fulde and K. Maki, Z. Phys. 238, 233 (1970).

[17]K. Aoi, Z. Phys. 246, 71 (1971); Z. Phys. 258, 284(E) (1973).

[18]T. Aomine and L. Rinderer, J. Low Temp. Phys. 10, 527 (1973).

[19]M. Strongin and O. F. Kammerer, Phys. Rev. Lett.

16, 456 (1966).
[20]P. M. Tedrow, R. Meservey, and B. B. Schwartz, Phys. Rev. Lett. 24, 1004 (1970).
[21]K. Aoi, R. Meservey, and P. M. Tedrow, Phys. Rev. B 7, 554 (1973).
[22]See the erratum in Ref. 17 and also Sec. II of the present work.
[23]A. A. Abrikosov and L. P. Gor'kov, Zh. Eksp. Teor. Fiz. 39, 1781 (1960) [Sov. Phys.-JETP 12, 1243 (1961)].
[24]Equation (19) is valid only for $H_{c\parallel} \gg H_{c\perp}$, which is always the case for very thin aluminum films. In the extreme type-II superconductors we expect that $H_c(\theta)$ (as well as bulk H_c) is limited by Pauli paramagnetism for all θ, so that $H_c(\theta) \approx$ const and $\theta_t = 90°$ [for a bulk case, see, for example, R. R. Hake, Phys. Rev. 158, 356 (1967)]. While this is an interesting case, we do not consider it in the present work.
[25]G. Hass, Z. Anorg. Allg. Chem. 254, 96 (1947).
[26]G. Hass, J. Opt. Soc. Am. 39, 532 (1949).
[27]P. M. Tedrow and R. Meservey, Phys. Rev. B 8, 5098 (1973).
[28]R. F. Hassing, R. R. Hake, and L. J. Barnes, Phys. Rev. Lett. 30, 6 (1973).
[29]M. K. Chien and R. E. Glover, III, in *Proceedings of the Thirteenth International Conference on Low Temperature Physics, Boulder, Colo.*, 1972, edited by R. H. Kropschot and K. D. Timmerhaus (University of Colorado Press, Boulder, Colo., 1973).

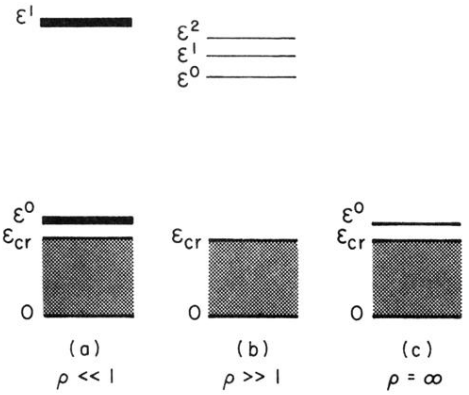

FIG. 3. Energy spectra of fluctuating pairs. This diagram illustrates the importance of the Landau quantization due to the perpendicular component of the magnetic field. ϵ^0 is the lowest energy level for the pairs; ϵ_{cr} is its critical value for superconductivity, that is, when $\epsilon^0 = \epsilon_{cr}$ is satisfied, the superconducting transition occurs. ϵ^n, $n = 1, 2 \ldots$ are other Landau levels. If $\rho \ll 1$ [case (a)] (corresponding to $\epsilon^0 - \epsilon_{cr} \ll \epsilon^0 - \epsilon'$), more thermal fluctuations occur at the lowest energy states than in the case of continuous distribution [case (c)] of states, because of the large degeneracy at this level in the former case. For $\rho \gg 1$ [case (b), the spectrum is almost a continuum and the discreteness is not important.

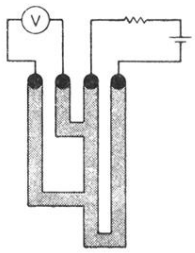

FIG. 6. Diagram showing sample shape. The width of the photoetched lines is 0.8 mm.